Title : will be set by the publisher
Editors : will be set by the publisher
EAS Publications Series, Vol. ?, 2005

FINITE RANK APPROXIMATION BASED METHOD FOR SOLVING THE RTE IN STELLAR ATMOSPHERES AND APPLICATION TO AN INVERSE PROBLEM

Axel Osses[1, 2] and Olivier Titaud[3]

Abstract. The Finite Rank Approximation (FRA) based method is well known in operator approximation theory but it is also useful for suggesting numerical methods for solving integral equations. In this document we describe two FRA methods for the numerical resolution of the integral formulation of the 1D Radiative Transfer Equation (RTE) posed in a static slab; we browse some advantages of them (especially the possibility to control the error) and we give some reduction of computation technics (iterative refinement schemes) which can be used with these methods. Numerical results obtained for a realistic Sun atmosphere model are given. In the last section we give an example of an inverse problem associated to the RTE: we show the iterative recovering of the albedo from the measurement of the outgoing specific intensity at a surface of the considered domain.

1 The transfer equation in stellar atmospheres

We consider a simplified 1D steady-state transfer equation posed in a static slab, stratified in plane-parallel homogeneous layers (Mihalas 1970): for all $\tau \in]0, \tau_\star[$ and all $\mu \in [-1, 1]$,

$$\mu \frac{\partial I}{\partial \tau}(\tau, \mu) = I(\tau, \mu) - \frac{\varpi(\tau)}{2} \int_{-1}^{1} I(\tau, \mu')\, d\mu' - S_\star(\tau), \tag{1.1}$$

The first author acknowledges FONDECYT 1030808 and ECOS CO4E08 grants. The second author acknowledges the support of ECOS-*Sud* postdoctoral grants: `www.ecos.univ-paris5.fr`. The authors are grateful to Bernard Rutily (Centre de Recherche Astronomique de Lyon, France) for fruitful discussion on this topic.

[1] Departamento de Ingeniería Matemática Universidad de Chile, Blanco Encalada 2120, Santiago de Chile, Chile; e-mail: `axosses@dim.uchile.cl`

[2] Centro de Modelamiento Matemático UMI 2807 CNRS, Universidad de Chile, Blanco Encalada 2120, Santiago de Chile, Chile

[3] Centro de Modelamiento Matemático UMI 2807 CNRS, Universidad de Chile, Blanco Encalada 2120, Santiago de Chile, Chile; e-mail: `titaud@dim.uchile.cl`

DOI: (will be inserted later)

where I, ϖ and $S_\star$ denote the *specific intensity*, the *albedo* and the *primary creation rate* respectively. The position variable τ is the optical depth at a given frequency, whose maximum value $\tau_\star$ is the optical thickness of the atmosphere. The cosine of the angle of incidence (zenith angle) is denoted by μ. We suppose moreover that we know the specific intensity of the incoming radiation on both boundary planes, i.e.

$$\left\{ \begin{array}{lcll} I(0,\mu) & = & I_0^-(\mu) & -1 \leq \mu < 0, \\ I(\tau_\star,\mu) & = & I_\star^+(\mu) & 0 < \mu \leq 1, \end{array} \right. \tag{1.2}$$

where I_0^- and $I_\star^+$ are given functions (see Figure 8a section 5). We define the *source function* by

$$S(\tau) = S_\star(\tau) + \frac{\varpi(\tau)}{2} \int_{-1}^{1} I(\tau,\mu)\, d\mu, \qquad \tau \in [0,\tau_\star]. \tag{1.3}$$

By injecting (1.3) in (1.1) we get an expression of I in terms of S and the boundary values I_0^- and $I_\star^+$: for all $\tau \in [0,\tau_\star]$,

$$I(\tau,\mu) = \left\{ \begin{array}{ll} I_0^-(\mu) \exp\left[\dfrac{\tau}{\mu}\right] - \dfrac{1}{\mu}\displaystyle\int_0^\tau S(s) \exp\left[\dfrac{\tau - s}{\mu}\right] ds, & \mu < 0, \\ S(\tau), & \mu = 0, \\ I_\star^+(\mu) \exp\left[-\dfrac{\tau_\star - \tau}{\mu}\right] + \dfrac{1}{\mu}\displaystyle\int_\tau^{\tau_\star} S(s) \exp\left[-\dfrac{s - \tau}{\mu}\right] ds, & \mu > 0. \end{array} \right. \tag{1.4}$$

The source function satisfies the following weakly integral equation

$$S(\tau) = S_0(\tau) + \frac{\varpi(\tau)}{2} \int_0^{\tau_\star} E_1(|\tau - \sigma|) S(\sigma)\, d\sigma, \qquad \tau \in [0,\tau_\star], \tag{1.5}$$

where the free term S_0 is given for all $\tau \in [0,\tau_\star]$ by

$$S_0(\tau) = S_\star(\tau) + \frac{\varpi(\tau)}{2} \left(\int_{-1}^{0} I_0^-(\mu) \exp(\tau/\mu)\, d\mu + \int_0^1 I_\star^+(\mu) \exp[-(\tau_\star - \tau)/\mu]\, d\mu \right). \tag{1.6}$$

The kernel E_1 is the first element of the exponential integral functions family $(E_k)_{k\geq 1}$ (Gradshteyn & Ryzhik 2000); these functions are defined for all $\tau > 0$ if $k = 1$ and for all $\tau \geq 0$ if $k > 1$ by

$$E_k(\tau) = \int_0^1 \exp(-\tau/\mu) \mu^{k-2}\, d\mu \quad k \geq 1. \tag{1.7}$$

E_1 is a weakly singular function at zero, i.e. it is singular at zero but it remains integrable on $[0,\tau_\star]$. Equation (1.5) belongs to a larger class of equations named *Fredholm integral equations*.

2 The FRA methods

The finite rank approximate (FRA) method is a very general method useful for operators approximations. It is used in spectral analysis but it can also be used to suggest and study some numerical methods for integral or partial differential equations (Ahues *et al.* 2001).

2.1 The RTE involves two operators

Equation (1.5) involves *two functional operators* acting on the unknown function S: the *identity operator*, denoted I, and an *integral operator* T defined by

$$(TS)(\tau) = \frac{\varpi(\tau)}{2} \int_0^{\tau_\star} E_1(|\tau - \sigma|) S(\sigma)\, d\sigma, \quad \tau \in [0, \tau_\star]. \tag{2.1}$$

Once we note this, we can remark that equation (1.5) can be written as

$$(I - T)S = S_0. \tag{2.2}$$

Remark on notations. In the astrophysical literature, it is usual to introduce the lambda operator as defined by $(\Lambda S)(\tau) = \frac{1}{2} \int_0^{\tau_\star} E_1(|\tau - \sigma|) S(\sigma) d\sigma$ and then $T = \varpi\Lambda$.

Solvability of the integral equation. It is of importance to know if an equation admits a solution and if it is unique or not. If

$$\sup_{\tau \in [0,\tau_\star]} \{|\varpi(\tau)|\} \times \left(1 - E_2\left(\frac{\tau_\star}{2}\right)\right) < 1, \tag{2.3}$$

then Equation (2.2) admits a unique solution for each S_0, which continuously depends on it (Titaud 2001). For example, as $E_2\left(\frac{\tau_\star}{2}\right) < 1$, this condition is satisfied if the albedo is less than or equal to one within the slab.

2.2 The two main ideas of the FRA methods

FRA methods are based on two main ideas. The first one is to replace into the original equation the exact operator T by an approximate one T_n, where n refers to some accuracy. We denote by S_n the solution of the corresponding approximate equation, which is

$$(I - T_n)S_n = S_0. \tag{2.4}$$

The second and main idea is to choose T_n as a finite rank operator, that is an operator whose image set is of finite rank: the image of a function S_n by such operator is a finite linear combination of a family of given functions, i.e.

$$T_n S_n = \sum_{j=1}^{n} \mathsf{x}_n(j) e_{n,j}. \tag{2.5}$$

Then, once the coefficients $\mathsf{x}_n(j)$, $1 \leq j \leq n$, are determined (see below), from (2.4) we get the following very important statement to recover S_n:

$$S_n = \sum_{j=1}^{n} \mathsf{x}_n(j) e_{n,j} + S_0. \tag{2.6}$$

Before browsing the general case, we give in the following sections two ways to construct such an operator T_n and the corresponding way to compute the coefficients $\mathsf{x}_n(j)$, $1 \leq j \leq n$.

Solvability of the approximate solution. If T_n is close enough to T (in some sense), then equation (2.4) admits a unique solution (Ahues *et al.* 2001).

2.2.1 First example: product integration based operator

Construction of T_n. Let us define a discretization grid on $[0, \tau_\star]$:

$$0 = \tau_0 < \tau_1 \cdots < \tau_{n-1} < \tau_n = \tau_\star. \tag{2.7}$$

Then the statement $TS_n(\tau) = \sum_{j=1}^{n} \dfrac{\varpi(\tau)}{2} \displaystyle\int_{\tau_{j-1}}^{\tau_j} E_1(|\tau - \sigma|) S_n(\sigma)\, d\sigma$ and an extended integral mean value theorem suggest the following approximation:

$$(TS_n)(\tau) \approx \sum_{j=1}^{n} S_n(\tau_j) \frac{\varpi(\tau)}{2} \int_{\tau_{j-1}}^{\tau_j} E_1(|\tau - \sigma|)\, d\sigma. \tag{2.8}$$

Consequently, we define T_n as

$$(T_n S_n)(\tau) = \sum_{j=1}^{n} S_n(\tau_j) \frac{\varpi(\tau)}{2} \int_{\tau_{j-1}}^{\tau_j} E_1(|\tau - \sigma|)\, d\sigma, \tag{2.9}$$

and finally we identify

$$\mathsf{x}_n(j) = S_n(\tau_j), \tag{2.10}$$

$$e_{n,j}(\tau) = \frac{\varpi(\tau)}{2} \int_{\tau_{j-1}}^{\tau_j} E_1(|\tau - \sigma|)\, d\sigma. \tag{2.11}$$

Note that the integral term in (2.11) can be expressed in terms of E_2 (Titaud 2001).

Determination of the entries $\mathsf{x}_n(j)$. In this case, we remark that the coefficient $\mathsf{x}_n(j)$ of the linear combination (2.5) corresponds to the evaluation of S_n at the node τ_j (this is not always the case, as we will see in the next example). To get an equation for these entries, we evaluate both members of the approximate equation (2.4) at each node τ_i: for all $1 \leq i \leq n$, we have

$$S_n(\tau_i) - (T_n S_n)(\tau_i) = S_0(\tau_i), \tag{2.12}$$

that is, following definition (2.10) of $\mathsf{x}_n(i)$,

$$\mathsf{x}_n(i) - \sum_{j=1}^{n} \mathsf{x}_n(j) e_{n,j}(\tau_i) = S_0(\tau_i). \tag{2.13}$$

If we define

$$\mathsf{A}_n(i,j) = e_{n,j}(\tau_i) = \frac{\varpi(\tau_i)}{2} \int_{\tau_{j-1}}^{\tau_j} E_1(|\tau_i - \sigma|)\, d\sigma, \tag{2.14}$$

$$\mathsf{b}_n(i) = S_0(\tau_i), \tag{2.15}$$

Equations (2.13) can be written as the linear system

$$(\mathsf{I}_n - \mathsf{A}_n)\mathsf{x}_n = \mathsf{b}_n, \tag{2.16}$$

where I_n denotes the identity matrix of order n. Once this system is solved (see section 4 later), we get from (2.6) and (2.11)

$$S_n(\tau) = \frac{\varpi(\tau)}{2} \sum_{j=1}^{n} \mathsf{x}_n(j) \int_{\tau_{j-1}}^{\tau_j} E_1(|\tau - \sigma|)\, d\sigma + S_0(\tau), \quad \tau \in [0, \tau_\star]. \tag{2.17}$$

One remarks that this way to construct T_n is natural because it involves the values of the approximate solution S_n at the nodes of the grid. But this aspect hides a bad feature: this method does not converge uniformly (Largillier & Titaud 2002), i.e. the speed of the convergence at a point depends on it. With a uniform convergence, the approximate solution converges at the same speed at all point, which is very useful to get better approximations. In the following example (projection based method) we construct a uniformly convergent method.

2.2.2 Second example: a projection based method

Construction of T_n. Let us define a grid of $n \geq 2$ nodes on $[0, \tau_\star]$ by

$$0 = \tau_1 < \tau_2 < \cdots < \tau_{n-1} < \tau_n = \tau_\star. \tag{2.18}$$

We approach TS_n by piecewise affine interpolations, as shown in Figure 1.

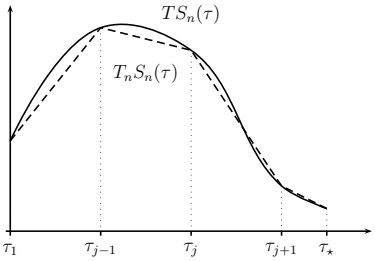

Fig. 1. Piecewise affine interpolation (dashed) of TS_n (solid).

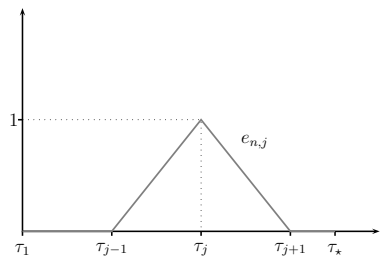

Fig. 2. Hat function.

Between two nodes, that is, for all $\tau \in [\tau_j, \tau_{j+1}]$, $1 \leq j \leq n-1$ we have

$$T_n S_n(\tau) = (TS_n)(\tau_j) + \frac{(TS_n)(\tau_{j+1}) - (TS_n)(\tau_j)}{\tau_{j+1} - \tau_j}(\tau - \tau_j). \tag{2.19}$$

Introducing the *characteristic functions* of the intervals $[\tau_j, \tau_{j+1}]$, $1 \leq j \leq n-1$,

$$\text{for all } \tau \in [0, \tau_\star], \qquad \mathbb{1}_{[\tau_j, \tau_{j+1}]}(\tau) = \begin{cases} 1 \text{ if } \tau \in [\tau_j, \tau_{j+1}], \\ 0 \text{ otherwise,} \end{cases} \tag{2.20}$$

we expand expression (2.19) for all $\tau \in [0, \tau_\star]$:

$$\begin{aligned}
T_n S_n(\tau) &= \sum_{j=1}^{n-1} \left[(TS_n)(\tau_j) + \frac{(TS_n)(\tau_{j+1}) - (TS_n)(\tau_j)}{\tau_{j+1} - \tau_j}(\tau - \tau_j) \right] \cdot \mathbb{1}_{[\tau_j, \tau_{j+1}]}(\tau) \\
&= \sum_{j=1}^{n-1} (TS_n)(\tau_j) \frac{\tau_{j+1} - \tau}{\tau_{j+1} - \tau_j} \cdot \mathbb{1}_{[\tau_j, \tau_{j+1}]}(\tau) \\
&+ \sum_{j=1}^{n-1} (TS_n)(\tau_{j+1}) \frac{\tau - \tau_j}{\tau_{j+1} - \tau_j} \cdot \mathbb{1}_{[\tau_j, \tau_{j+1}]}(\tau) \\
&= \sum_{j=1}^{n-1} (TS_n)(\tau_j) \frac{\tau_{j+1} - \tau}{\tau_{j+1} - \tau_j} \cdot \mathbb{1}_{[\tau_j, \tau_{j+1}]}(\tau) \\
&+ \sum_{j=2}^{n} (TS_n)(\tau_j) \frac{\tau - \tau_{j-1}}{\tau_j - \tau_{j-1}} \cdot \mathbb{1}_{[\tau_{j-1}, \tau_j]}(\tau) \\
&= (TS_n)(\tau_1) \frac{\tau_2 - \tau}{\tau_2 - \tau_1} \cdot \mathbb{1}_{[\tau_1, \tau_2]}(\tau) + (TS_n)(\tau_n) \frac{\tau - \tau_{n-1}}{\tau_n - \tau_{n-1}} \cdot \mathbb{1}_{[\tau_{n-1}, \tau_n]}(\tau) \\
&+ \sum_{j=2}^{n-1} (TS_n)(\tau_j) \left[\frac{\tau - \tau_{j-1}}{\tau_j - \tau_{j-1}} \cdot \mathbb{1}_{[\tau_{j-1}, \tau_j]}(\tau) + \frac{\tau_{j+1} - \tau}{\tau_{j+1} - \tau_j} \cdot \mathbb{1}_{[\tau_j, \tau_{j+1}]}(\tau) \right].
\end{aligned} \tag{2.21}$$

If we define the family $(e_{n,j})_{j=1}^n$ of piecewise affine functions — so called *hat functions* (see Figure 2 above) — by

$$e_{n,1}(\tau) = \frac{\tau_2 - \tau}{\tau_2 - \tau_1} \cdot \mathbb{1}_{[\tau_1, \tau_2]}(\tau), \quad \tau \in [0, \tau_\star], \tag{2.22}$$

$$e_{n,n}(\tau) = \frac{\tau - \tau_{n-1}}{\tau_n - \tau_{n-1}} \cdot \mathbb{1}_{[\tau_{n-1}, \tau_n]}(\tau), \quad \tau \in [0, \tau_\star], \tag{2.23}$$

and for $2 \leq j \leq n-1$

$$e_{n,j}(\tau) = \frac{\tau - \tau_{j-1}}{h_j} \mathbb{1}_{[\tau_{j-1}, \tau_j]}(\tau) + \frac{\tau_{j+1} - \tau}{h_{j+1}} \mathbb{1}_{[\tau_j, \tau_{j+1}]}(\tau), \quad \tau \in [0, \tau_\star], \tag{2.24}$$

where

$$h_j = \tau_j - \tau_{j-1}, \quad 2 \leq j \leq n, \tag{2.25}$$

then Equality (2.21) becomes

$$(T_n S_n)(\tau) = \sum_{j=1}^{n} (TS_n)(\tau_j) e_{n,j}(\tau). \tag{2.26}$$

Finally, identifying

$$\mathsf{x}_n(j) = (TS_n)(\tau_j), \tag{2.27}$$

we get the general form (2.5) which allows us to look at T_n as a finite rank operator.

Determination of the entries $\mathsf{x}_n(j)$. In this case, we remark that the coefficient $\mathsf{x}_n(j)$ of the linear combination (2.5) corresponds to the evaluation of (TS_n) at the node τ_j. In order to get equations for these entries, we apply T on both members of equation (2.4) before evaluating them at each node τ_i. We get, for all $1 \leq i \leq n$,

$$(TS_n)(\tau_i) - [T(T_n S_n)](\tau_i) = (TS_0)(\tau_i), \tag{2.28}$$

$$(TS_n)(\tau_i) - \sum_{j=1}^{n} \mathsf{x}_n(j)(Te_{n,j})(\tau_i) = (TS_0)(\tau_i). \tag{2.29}$$

If we define

$$\mathsf{A}_n(i,j) = (Te_{n,j})(\tau_i) = \frac{\varpi(\tau_i)}{2} \int_0^{\tau_\star} E_1(|\tau_i - \sigma|) e_{n,j}(\sigma)\, d\sigma, \tag{2.30}$$

$$\mathsf{b}_n(i) = (TS_0)(\tau_i) = \frac{\varpi(\tau_i)}{2} \int_0^{\tau_\star} E_1(|\tau_i - \sigma|) S_0(\sigma)\, d\sigma, \tag{2.31}$$

and if we take into account definition (2.27) of x_n, Equations (2.29) can be written as the linear system

$$(\mathsf{I}_n - \mathsf{A}_n)\mathsf{x}_n = \mathsf{b}_n. \tag{2.32}$$

Once this system is solved (see section 4), we get from (2.6)

$$S_n = \sum_{j=1}^{n} \mathsf{x}_n(j) e_{n,j} + S_0, \tag{2.33}$$

where $(e_{n,j})_{j=1}^{n}$ are defined by (2.22)-(2.24). The entries of the matrix A_n defined by (2.30) can be expressed in terms of the exponential integral functions E_2 and E_3 (Titaud 2001). One can notice that these entries do not correspond to the values of the approximate solution S_n at the nodes of the grid but to the value of the image of it by the exact operator T. This method is uniformly convergent, contrary to the product integration method described above.

Remarks. This method uses affine interpolations but it can be generalized to polynomial interpolations of higher order (Ahues *et al.* 2001).

2.2.3 General case

Suppose that we have constructed an approximate operator T_n with a given family of basis functions $(e_{n,j})_{j=1}^n$, i.e. such that

$$T_n S_n = \sum_{j=1}^{n} \mathsf{x}_n(j) e_{n,j}. \tag{2.34}$$

From the two previous examples, it is clear that the coefficients $\mathsf{x}_n(j)$ of the linear combination depend linearly on S_n. Then $\mathsf{x}_n(j)$ is a real valued linear function of S_n and we will write

$$\mathsf{x}_n(j) = \ell_{n,j}(S_n), \tag{2.35}$$

which gives in the definition of T_n:

$$T_n S_n = \sum_{j=1}^{n} \ell_{n,j}(S_n) \times e_{n,j}. \tag{2.36}$$

The approximate equation (2.4) becomes

$$S_n - \sum_{j=1}^{n} \ell_{n,j}(S_n) \times e_{n,j} = S_0. \tag{2.37}$$

Now, if we apply $\ell_{n,i}$, $i = 1 \dots n$, on both members of the previous equality, we get

$$\ell_{n,i}(S_n) - \sum_{j=1}^{n} \ell_{n,j}(S_n) \times \ell_{n,i}(e_{n,j}) = \ell_{n,i}(S_0), \quad 1 \le i \le n. \tag{2.38}$$

If we set finally

$$\mathsf{A}_n(i,j) = \ell_{n,i}(e_{n,j}), \qquad \mathsf{b}_n(i) = \ell_{n,i}(S_0), \tag{2.39}$$

it is clear that equalities (2.38), which are valid for all $i = 1 \dots n$, can be written as the following linear system

$$(\mathsf{I}_n - \mathsf{A}_n)\mathsf{x}_n = \mathsf{b}_n, \tag{2.40}$$

where I_n denotes the identity matrix of order n. In the following A_n is called *matrix of the discretized problem*. Once this system is solved, we get S_n by (2.35) and (2.37):

$$S_n(\tau) = \sum_{i=1}^{n} \mathsf{x}_n(i) e_{n,i}(\tau) + S_0(\tau), \qquad \tau \in [0, \tau_\star]. \tag{2.41}$$

It is important to notice that S_n is known all over $[0, \tau_\star]$. We have got an expression of S_n in terms of τ which allows us to compute some integrals where S_n is involved without other approximations: for instance, we can inject S_n in the solution (1.4) to get an approximation of the specific intensity (see the numerical experiment section 5). This feature is also useful in the error analysis (see the next section). In the case of product integration method, from (2.10) and (2.35), we identify $\ell_{n,i}(S_n) = S_n(\tau_i)$. Similarly, in the case of projection method, from (2.27) and (2.35), we identify $\ell_{n,i}(S_n) = (TS_n)(\tau_i)$.

3 Error analysis

FRA methods give us an approximate solution S_n of the exact one S. In order to know if the approximation is close to the solution, we need to estimate the difference

$$e_n = S_n - S. \tag{3.1}$$

We call this error the *discretization error* because it comes from the method used to approach the original problem by a discretization method — the subscript n refers to it. Except for some particular cases where the solution of (1.5) is known (Rutily & Bergeat 1994), it is obviously impossible to compute e_n. We need then to find other ways to evaluate the quality of the approximate solution.

3.1 Error bounds

Any good numerical method provides a bound M_n of the error

$$\|e_n\| = \|S_n - S\| \leq M_n, \tag{3.2}$$

which generally depends on the discretization method, on some parameters of the problem and on the largest grid step of the discretization grid

$$h = \max_{2\leq j\leq n} |\tau_j - \tau_{j-1}|. \tag{3.3}$$

For FRA methods applied to problem (1.5) we have $M_n = M_n(\tau_\star, \varpi, E_1, h)$. The norm $\|\cdot\|$ must be chosen accordingly to the functional space which S and S_n belong to. This technical aspect will not be detailed and we will assume that the norm is the usual one in the space of continuous functions, i.e.

$$\|S\| = \sup_{\tau\in[0,\tau_\star]} |S(\tau)|. \tag{3.4}$$

This norm is called *infinity norm* or *uniform norm*. The first way to control the error is then to fix the parameters of the numerical method in order to get M_n as smaller as we want. But, in some cases these bounds can not be used in practice because there are too pessimistic (Ahues *et al.* 2002). Some relative error bounds for the FRA methods described above are given in (Ahues *et al.* 2002; Titaud 2001).

3.2 Residuals

Another way to evaluate the quality of an approximate solution S_n is to estimate the *discretization residual*, which is defined by

$$r_n = (I - T)S_n - S_0, \tag{3.5}$$

where the subscript n also refers to the discretization method. This function estimates how the approximate solution S_n solves the exact equation (2.2) *at each point of the interval*. A small residual means that $(I - T)S_n$ effectively predicts the right-hand side S_0.

3.2.1 The residual equation

As problem (2.2) is linear, any error e on the exact solution satisfies the same equation as the unknown S when the second member S_0 is replaced by the corresponding residual r. This important relationship is called the *residual equation*:

$$(I - T)e = r. \tag{3.6}$$

We can derive it by noting that the residual associated with the exact solution S is zero: $(I - T)S - S_0 = 0$. This equation is the key of *residual correction technic* whose aim is to refine some approximate solutions (see section 4). If we define the norm of the operator T by

$$\|T\| = \sup\{\|Tx\|, \quad \|x\| = 1\}, \tag{3.7}$$

and if we suppose that $(I-T)$ is invertible (that is, equation (2.2) admits a unique solution), from (3.6) and the well known inequality $\|(I - T)^{-1}\| \leq 1/(1 - \|T\|)$, we can derive a first bound for the error in terms of the residual:

$$\|e\| \leq \frac{1}{1 - \|T\|}\|r\|. \tag{3.8}$$

There is another way to know how the residual measures the error in terms of the *condition number* of the operator $(I - T)$, defined by

$$\kappa(I - T) = \|I - T\| \times \|(I - T)^{-1}\| \geq 1. \tag{3.9}$$

On the first hand, noting that $(I - T)e = r$ and $S = (I - T)^{-1}S_0$, we get $\|r\| \leq \|I - T\| \times \|e\|$ and $1/\|S_0\| \leq \|(I - T)^{-1}\|/\|S\|$. On the second hand, using the inverse relations $e = (I-T)^{-1}r$ and $(I-T)S = S_0$, we get $\|e\| \leq \|(I-T)^{-1}\| \times \|r\|$ and $1/\|S\| \leq \|I - T\|/\|S_0\|$. Mixing these two inequalities we get

$$\frac{1}{\kappa(I - T)}\frac{\|r\|}{\|S_0\|} \leq \frac{\|e\|}{\|S\|} \leq \kappa(I - T)\frac{\|r\|}{\|S_0\|}. \tag{3.10}$$

For example, suppose that we have reached a relative residual $\|r\|/\|S_0\| = 10^{-2}$. If the condition number is large, for instance $\kappa(I-T) = 10^5$, then we have $10^{-7} \leq \|e\|/\|S\| \leq 10^3$: the relative error can be large although the relative residual is small. If the condition number is small, say $\kappa(I-T) = 10$, then $10^{-3} \leq \|e\|/\|S\| \leq 10^{-1}$ and the relative error is necessarily small.

3.2.2 Case of the projection method

Suppose that $S_0 = \sum_{j=1}^{n} \mathsf{s}_n(j)e_{n,j}$. Then we get the following expression of the discretization residual of the approximate solution (2.33) of problem (1.5) given by the projection based method: for all $\tau \in [0, \tau_\star]$, we have

$$r_n(\tau) = \sum_{j=1}^{n}(\mathsf{y}_n(j) - \mathsf{s}_n(j))e_{n,j}(\tau) - \mathsf{y}_n(j)\frac{\varpi(\tau)}{2}\int_0^{\tau_\star} E_1(|\tau - \sigma|)e_{n,j}(\sigma)\, d\sigma. \tag{3.11}$$

It is important to notice that since the above integrals have got an expression in terms of E_2 and E_3, it is possible to compute the discretization residual *for all* $\tau \in [0, \tau_\star]$.

4 Resolution of the linear system

4.1 Global error

FRA methods, as quite all numerical methods, involve the resolution of a linear system and then suffer from the impossibilities to compute exactly the entries of the discretization matrix A_n and to compute exactly the solution of the system $(\mathsf{I}_n - \mathsf{A}_n)\mathsf{x}_n = \mathsf{b}_n$. Let us denote by $\widehat{\mathsf{x}}_n$ the computed solution of the linear system (2.40) and $\widehat{S}_n$ the corresponding approximation of S_n, i.e.

$$\widehat{S}_n = \sum_{j=1}^{n} \widehat{\mathsf{x}}_n(j) e_{n,j} + S_0. \tag{4.1}$$

Then, the numerical method used to solve the linear system will add the following *computation error*:

$$\widehat{e} = \widehat{S}_n - S_n = \sum_{j=1}^{n} (\widehat{\mathsf{x}}_n - \mathsf{x}_n)(j) e_{n,j}, \tag{4.2}$$

and finally we get the following bound for the *global error* $e = \widehat{S}_n - S$ in the numerical resolution of the transfer equation with a FRA method (or any numerical methods which involves the resolution of a linear system):

$$\|e\| \leq \|\widehat{e}\| + \|e_n\|. \tag{4.3}$$

To get a coherent final approximation, one should choose a linear system solver which ensures a computation error $\|\widehat{e}\|$ of the order of the discretization error $\|e_n\|$. In other words, *it is useless to use a sophisticated system solver if the discretization error remains large.* The associated *global residual* is given by:

$$r = (I - T)\widehat{S}_n - S_0 = \sum_{j=1}^{n} \widehat{\mathsf{x}}_n(j)(I - T)e_{n,j} - TS_0. \tag{4.4}$$

It is linked with the global error by the residual equation (3.6). Remark that generally the inequality $\|r\| \leq \|\widehat{r}\| + \|r_n\|$ does not hold, where $\widehat{r} = (I - T_n)\widehat{S}_n - S_0$ is the *computation residual*, i.e. the residual of $\widehat{S}_n$ with respect to the approximate equation $(I - T_n)S_n = S_0$. Indeed we have

$$r = (I - T)(\widehat{e} + e_n) = (I - T_n)\widehat{e} + (T_n - T)\widehat{e} + r_n = (T_n - T)\widehat{e} + \widehat{r} + r_n.$$

4.2 Gaussian Elimination method for dense unstructured linear systems

The choice of the numerical method to solve a linear system highly depends on the structure of the corresponding matrix. Almost all numerical methods for integral equations involve the resolution of a square *dense* linear system and FRA methods have got this feature. Moreover, if the discretization grid is not uniform or if the albedo is not constant, this system is unstructured. Figure 3 shows an example of such a discretization matrix for a non-uniform grid and a variable albedo.

i	1	2	3	4	5
τ_i	$0,0$	$0,1$	$1,0$	$4,0$	$7,445$
$\varpi(\tau_i)$	$5,29.10^{-01}$	$3,27.10^{-03}$	$7,46.10^{-04}$	$3,98.10^{-04}$	$5,59.10^{-04}$

$$\mathsf{A}_n = \begin{bmatrix} 4,31.10^{-02} & 1,31.10^{-01} & 8,07.10^{-02} & 9,22.10^{-03} & 1,91.10^{-04} \\ 1,87.10^{-04} & 1,22.10^{-03} & 6,13.10^{-04} & 6,53.10^{-05} & 1,32.10^{-06} \\ 4,33.10^{-06} & 9,54.10^{-05} & 5,30.10^{-04} & 6,01.10^{-05} & 8,76.10^{-07} \\ 3,92.10^{-08} & 6,14.10^{-07} & 3,13.10^{-05} & 3,37.10^{-04} & 2,74.10^{-05} \\ 1,02.10^{-09} & 1,53.10^{-08} & 4,42.10^{-07} & 3,97.10^{-05} & 2,40.10^{-04} \end{bmatrix}$$

Fig. 3. Example of a discretization matrix for a non-uniform grid projection method and a variable albedo.

In their introduction to the Gaussian Elimination (GE) method (also known as the *LU decomposition method*), Golub & Van Loan (1996) say that it is "the algorithm of choice when [the matrix] is square, dense and unstructured". One can find in (Golub & Van Loan 1996) different implementations of GE based algorithms. A very complete error and stability analysis of GE with historical references can be found in (Higham 1996).

4.3 Iterative refinement

Description of Iterative Refinement (IR). Suppose we want to compute a very accurate approximation S_N, that is to solve the approximate equation

$$(I - T_N)S_N = S_0, \tag{4.5}$$

where the number of grid nodes N is very large. In order to attain this given precision, the largest grid step h_N will be so small that the dimension of the corresponding linear system (2.40) of rank N will be prohibitively large from a computational point of view.

Refinement schemes allow us to reach iteratively the exact solution of a large scale linear system by means of the resolution of a sequence of linear systems of moderate fixed size. This technic is often implemented with the LU decomposition method because the factorization of the matrix involved in the small system can be reused. Next, n refers to a coarse approximation, while the subscript N denotes a fine one. To understand the structure of the refinement schemes we

need to introduce the *resolvent operator* of the operator T involved in the integral equation (2.2):

$$R = (I - T)^{-1}. \tag{4.6}$$

Then the solution of equation $(I-T)S = S_0$ is given by $S = RS_0$. If we denote by R_n a coarse approximation of the exact resolvent operator R, then $S_n = R_n S_0$ is an approximation of S. Section 2.2 was devoted to describe how to construct such an approximate resolvent by the FRA method: we used $R_n = R_n^{(A)} = (I - T_n)^{-1}$ but it can be generalized (see below). The process of iterative refinement is based on the *residual correction technic* which consists in using the residual equation (3.6) to improve an approximate solution computed by a numerical method. The basic scheme is the following: let $S^{(0)}$ be an approximation of S; for $k = 0, 1, \ldots,$ do the following three steps:

$$\begin{array}{ll} \circ \text{ Compute the finest approx. residual} & r^{(k)} = (I - T_N)S^{(k)} - S_0 \\ \circ \text{ Solve the coarse residual equation} & e^{(k)} = R_n r^{(k)} \\ \circ \text{ Correct the approximation} & S^{(k+1)} = S^{(k)} - e^{(k)} \end{array} \tag{4.7}$$

The scheme should be stopped when the finest approximation relative residual $\|r^{(k)}\|/\|S_0\|$ is small enough.

Three iterative refinement schemes. The most elementary way to refine an approximate solution $S^{(0)}$ is to choose R_n equal to the resolvent of the approximate operator $(I-T_n)$ i.e., $R_n = R_n^{(A)} = (I-T_n)^{-1}$. The corresponding scheme is called *Atkinson scheme* (Atkinson 1976):

$$\left\{ \begin{array}{lcl} S^{(0)} & = & R_n^{(A)} S_0, \\ S^{(k+1)} & = & S^{(0)} + R_n^{(A)}(T_N - T_n)S^{(k)}, \quad k \geq 0. \end{array} \right. \tag{4.8}$$

Since the exact resolvent operator R satisfies the identities $R = RT + I = TR + I$, we may suggest two new approximations of R which are: $R_n^{(B)} = R_n^{(A)} T + I$ and $R_n^{(C)} = TR_n^{(A)} + I$. These approximate resolvent operators lead to the following schemes. The *Brakhage scheme* is given by (Atkinson 1976):

$$\left\{ \begin{array}{lcl} S^{(0)} & = & R_n^{(B)} S_0, \\ S_n^{(k+1)} & = & S^{(0)} + R_n^{(A)}(T_N - T_n)T_N S^{(k)}, \quad k \geq 0, \end{array} \right. \tag{4.9}$$

and the *C scheme* is given by (Ahues *et al.* 2002):

$$\left\{ \begin{array}{lcl} S^{(0)} & = & R_n^{(C)} S_0, \\ S^{(k+1)} & = & S^{(0)} + T_N R_n^{(A)}(T_N - T_n)S^{(k)}, \quad k \geq 0. \end{array} \right. \tag{4.10}$$

Remark that these schemes were rewritten in an equivalent way as (4.7) to avoid some unstabilities due to the convergence to zero of the residual. A brief comparison between non-stationary iterative methods and iterative refinement schemes

was performed on an example, where a projection method in the space $L^1([0,\tau_\star])$ was used, in (D'Almeida *et al.* 2003). Complete descriptions of the implementation of these schemes applied on problem (2.2) can be found in (Titaud 2001 ; D'Almeida *et al.* 2003) . Some numerical results about the behavior of these schemes with respect to $\tau_\star$ and ϖ are given in (Titaud 2001, Ahues *et al.* 2002). A parallelization of these algorithms is described in (Ahues *et al.* 2002).

4.4 Gain of computational and memory costs

Structure of the matrix of the discretized problem. As the kernel of the integral equation (1.5) decreases exponentially at infinity, *if $\tau_\star$ is large*, a lot of entries of the discretization matrix (2.30) are close to zero. Figure 4 shows the profile of this matrix for a projection method applied with a uniform grid of 100 elements on $[0, 100]$.

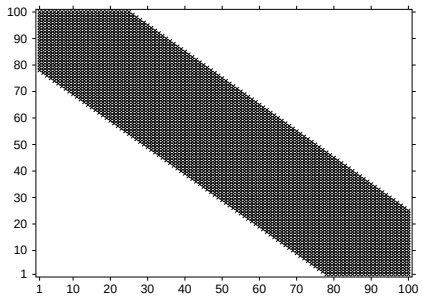

Fig. 4. Profile of a discretization matrix A_n. Only coefficients of modulus greater than 10^{-12} are plotted.

A trick to reduce memory and computational costs. A consistent way to *replace* by zero some small entries of the matrix A_n — in the case of a projection approximation — is suggested and justified in (Titaud 2004). The main idea is to truncate the kernel E_1 and to construct another approximate operator $\widetilde{T}_n$ in such a way that the corresponding matrix $\widetilde{\mathsf{A}}_n$ has got a band structure and that we can control the error $\|\widetilde{S}_n - S_n\|$ between the corresponding approximate solution $\widetilde{S}_n$ and the original discretized problem approximate solution S_n (without cancellation). Moreover the trick avoids the computation of the entries which may be replaced by zero: it permits us to know what entries will be small before computing them. In the case of a large matrix, we gain computation time and memory. The second point allows us to choose the error $\|\widetilde{S}_n - S_n\|$ at worst of the order of the discretization one $\|S - S_n\|$ which can be evaluated by mean of the residual (see section 3.2.1). Indeed, using the triangle inequality we have $\|\widetilde{S}_n - S\| \leq \|\widetilde{S}_n - S_n\| + \|S - S_n\|$.

Iterative methods to solve band linear system. The band matrix produced by the previous technic shows few non-zero off-diagonals and then iterative methods (like Jacobi, SOR, Gauss-Seidel, Krylov subspaces based methods, etc.) for solving the corresponding sparse system $(\widetilde{\mathsf{A}}_n - \mathsf{I}_n)\mathsf{x}_n = \widetilde{\mathsf{b}}_n$ should be used. Complete description of basic iterative methods can be found in (Golub & Van Loan

1996). For a good overview of practical iterative algorithms for solving large-scale linear sparse systems see (Saad 2003), especially for Krylov subspace technics. An accuracy and stability analysis is treated in (Higham 1996). Using iterative refinement to solve this kind of systems is also possible (D'Almeida *et al.* 2003).

Remarks on multigrid methods (MG). Jacobi and Gauss-Seidel iterations for solving linear system $\mathsf{A}\mathsf{x} = \mathsf{b}$ are both of the form $\mathsf{x}^{k+1} = \mathsf{G}\mathsf{x}^k + \mathsf{b}$. The matrix G is often called the *iteration matrix* (which is not the matrix A). We call *high frequency modes* or *oscillatory modes* the eigenvectors of the iteration matrix G which correspond to the largest eigenvalues of this matrix. The other eigenvectors (i.e. associated to the smallest eigenvalues) are called *low frequency modes* or *smooth modes*. During the iteration process, oscillatory components of the error (or of the residual), are rapidly eliminated while smooth ones are slowly reduced. This property, which is shared by the majority of standard iterative methods, is called the *smoothing property* (Briggs *et al.* 2000). *Multigrid methods* take advantage of the fact that a smooth error appears more oscillatory on a coarser grid than on a fine one, to overcome this problem. The main idea is to move to a coarser grid when the iterative scheme is stagnating. There is a noteworthy difference between IR schemes and MG methods: the last ones are based on iterative methods and then they are well suited for sparse systems and unsuitable for dense ones. IR are well suited for dense matrices and some kind of sparse ones (D'Almeida *et al.* 2003). Moreover MG methods start with an approximate solution given on a fine grid whereas IR schemes start with a coarse approximate solution. But both are based on the correction residual technic which takes advantage of the residual equation (3.6). A very good introduction to these methods can be found in (Briggs *et al.* 2000). A repository for information related to multigrid can be found in `www.mgnet.org`.

5 Numerical experiments in the Sun's atmosphere

Let us test the projection method described in section 2.2.2 on a realistic transfer calculation. We solved problem (1.5) in the solar atmosphere at $\lambda = 500$ nm. To derive the coefficients of the radiative transfer equation (1.1), we used the temperature, electronic and atomic hydrogen number densities as given by the model of Vernazza *et al.* (1981). This NLTE model includes the Sun's chromosphere and the beginning of the transition region, where the gradients are high, the albedo close to unity and the transfer equation difficult to solve (Rutily & Chevallier 2005). The opacity χ at $\lambda = 500$nm has been deduced from the corresponding tabulated optical depth and we have $\tau_\star = 7.445$. The scattering coefficient σ, which describes the Thomson scattering on free electrons and the Rayleigh scattering on hydrogen atoms, was calculated with the help of the tabulated electronic and atomic hydrogen number densities. Denoting by B_λ the Planck function at frequency λ, we deduced the albedo $\varpi = \sigma/\chi$ and the primary creation rate $S_\star = (1 - \varpi)B_\lambda(T)$, the temperature T being given by the model. Concerning the boundary conditions, we supposed no incoming radiation at the top surface ($I_0^-(\mu) = 0$) and we adopted

the diffusion approximation at the bottom surface: $I_0^+(\mu) = B_\lambda(\tau_*) + \mu dB_\lambda/d\tau(\tau_*)$.

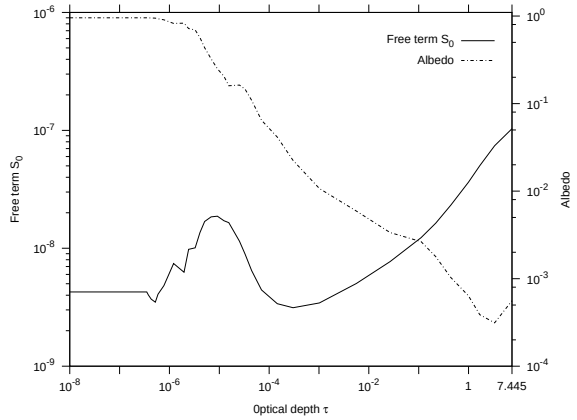

Fig. 5. Free term S_0 (solid) and albedo (dashed) — from Vernazza *et al.* (1981) NTLE model of the Sun atmosphere, $\lambda = 500$nm.

Figure 5 shows the free term S_0 (1.6) and the albedo ϖ involved in (1.5). Figure 6 shows the approximate source function S_n (2.33) constructed with the projection method described in section 2.2.2; the discretization grid is non-uniform and has $n = 33$ nodes: they correspond to some optical depths tabulated by the model. Note that the corresponding relative residual — drawn in the same Figure 6 — is very small (its maximum value is less than 10^{-6}), which shows that the projection method is able to solve realistic continuum radiative transfer problems. Figures 7a and 7b show an approximate specific intensity I_n for $\mu \leq 0$ and $\mu > 0$, respectively. It is deduced from replacing S by S_n into the solution (1.4). No other approximation is made here because the integrations over S_n can be performed in terms of exponential integral functions. This advantage comes from the fact that $S_n(\tau)$ is known for all $\tau \in [0, \tau_\star]$ (see section 2.2.3). ALI methods do not have this feature. From this model we deduce an approximation of the outgoing radiation specific intensity at the surface $\tau = 0$, that is we can compute $I_0^+(\mu) = I(0, \mu)$, for $0 < \mu \leq 1$. This quantity will be used in the inverse problem described in the next section.

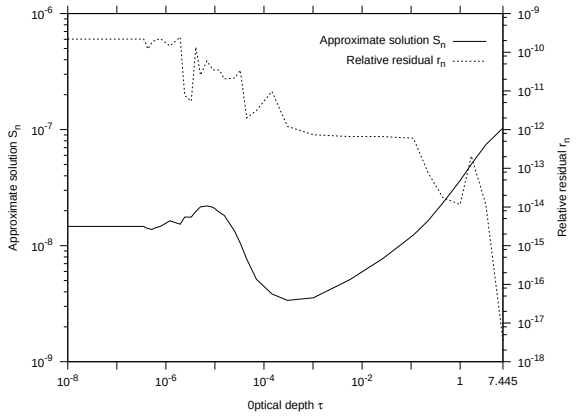

Fig. 6. Approximate source function S_n (solid) and its relative residual (dashed) computed with a projection method — from Vernazza *et al.* (1981) NTLE model of the Sun atmosphere, $\lambda = 500$nm.

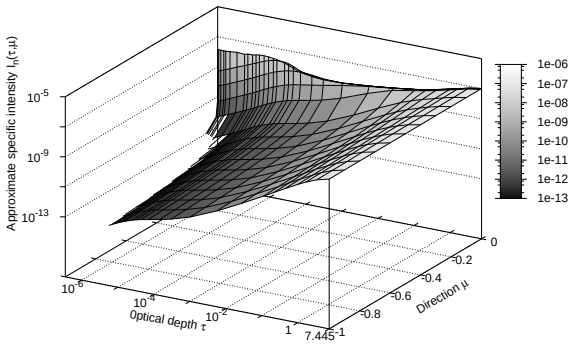

Fig. 7a. Approximate specific intensity for $\mu \leq 0$ computed from S_n and the solution (1.4) — from Vernazza *et al.* (1981) NTLE model of the Sun atmosphere, $\lambda = 500$nm.

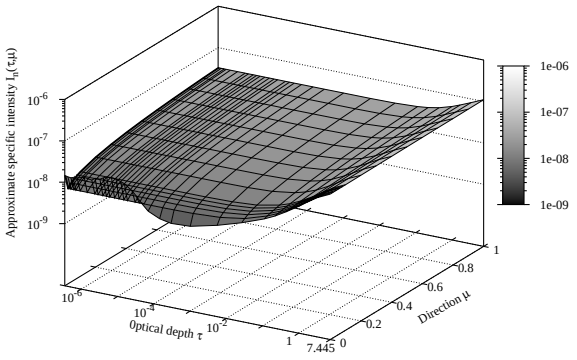

Fig. 7b. Approximate specific intensity for $\mu \geq 0$ computed from S_n and the solution (1.4) — from Vernazza *et al.* (1981) NTLE model of the Sun atmosphere, $\lambda = 500$nm.

6 Inverse problems

We consider here the following non-linear *inverse problem*: we want to recover the albedo — that we will denote by $\widetilde{\varpi}$ from now — in Equation (1.1) from the knowledge (i.e. the measurement) of the corresponding *Outgoing Radiation Specific Intensity* (ORSI) at the surface $\tau = 0$, i.e. from $\widetilde{I}(0,\mu)$, $0 < \mu \leq 1$. Up to now, we considered a *direct* radiative transfer problem: the aim was to compute the specific intensity I from the knowledge of the parameters $\tau_\star$, ϖ, $S_\star$ and of the *incoming radiation* $I_0^-(\mu)$, $-1 \leq \mu < 0$, and $I_\star^+(\mu)$, $0 < \mu \leq 1$ (see Figure 8a&b).

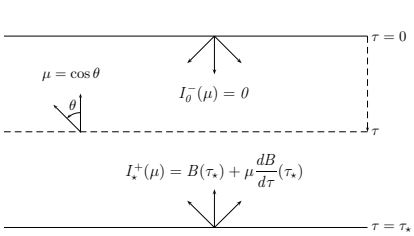

Fig. 8a. Direct problem:
$\varpi,\ I_0^-,\ I_\star^+ \longrightarrow I(\tau,\mu)$

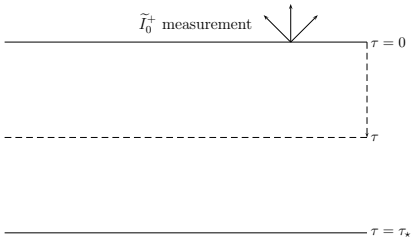

Fig. 8b. Inverse problem:
$\widetilde{I}_0^+ \longrightarrow \varpi$ (nonlinear)

We suppose that $\tau_\star$ is known and that $S_\star(\tau) = (1 - \varpi(\tau))B_\lambda(\tau)$: in the following numerical experiments, we use the same model of the last section. We

suppose that the target albedo $\widetilde{\varpi}$ is a piecewise affine function defined by

$$\widetilde{\varpi}(\tau) = \sum_{i=1}^{n} \widetilde{\mathsf{w}}_i e_{n,i}(\tau), \qquad \tau \in [0, \tau_\star], \tag{6.1}$$

where the family $(e_{n,i})_{i=1}^n$ is defined by (2.22)-(2.24) from a given fixed grid $(\tau_i)_{i=1}^n$. Then $\widetilde{\mathsf{w}}_i = \widetilde{\varpi}(\tau_i)$ are the entries of $\widetilde{\mathsf{w}}$, the vector value of $\widetilde{\varpi}$ on the previous grid. We define the ORSI on the boundary layer $\tau = 0$ for positive μ by:

$$I_0^+ \ : \mu \geq 0 \ \mapsto I(0, \mu), \tag{6.2}$$

where I is the solution of problem (1.1) with a given albedo ϖ, and we denote by $\mathcal{R}$ the *observational* or *response operator*

$$\mathcal{R} \ : \ \mathsf{w} \mapsto I_0^+, \tag{6.3}$$

where w is the vector value of ϖ on the grid $(\tau_i)_{i=1}^n$. The bijectivity of the map $\mathcal{R}$ is not obvious and it has not be studied in the case of equation (1.1) yet, but in the semi-space case (Bal 2000).

Our goal is to recover an approximation of $\widetilde{\mathsf{w}}$ from a finite number p of measurements of the corresponding ORSI $\widetilde{I}_0^+$. The idea (McCormick 1992) is to minimize the following quadratic error

$$Q(\mathsf{w}) = \frac{1}{2}(\mathsf{Y}(\mathsf{w}) - \widetilde{\mathsf{y}})^T \mathsf{R}(\mathsf{Y}(\mathsf{w}) - \widetilde{\mathsf{y}}) + \frac{1}{2}(\mathsf{w} - \bar{\mathsf{w}})^T \mathsf{B}(\mathsf{w} - \bar{\mathsf{w}}), \qquad \mathsf{w} \in \mathbb{R}^n, \tag{6.4}$$

where $\widetilde{\mathsf{y}} \in \mathbb{R}^p$ denotes the *observation vector* whose entries are $\widetilde{\mathsf{y}}_k = \mathcal{R}(\widetilde{\mathsf{w}})(\mu_k)$; $\mathsf{Y}(\mathsf{w}) \in \mathbb{R}^p$ is the vector of entries $\mathcal{R}(\mathsf{w})(\mu_k)$, $1 \leq k \leq p$; $\bar{\mathsf{w}}$ is a first guess of the target $\widetilde{\mathsf{w}}$; R and B are matrices whose role is to balance both members of Q. For the observation part of Q we choose $\mathsf{R}(k,l) = (\int_0^1 e_{p,k} e_{p,l}(\mu) d\mu)/\widetilde{\sigma}$, $1 \leq k, l \leq p$, where $\widetilde{\sigma}$ is a percentage of $|\widetilde{y}_p|$ which represents the variance of the error on the observations. The family of functions $(e_{p,k})_{k=1}^p$ are defined on $[0,1]$ from $(\mu_k)_{k=1}^p$ in an similar manner than in (2.22)-(2.23)-(2.24). The weights on the parameter part of Q are chosen as $\mathsf{B}(i,j) = \sigma_i \sigma_j (\int_0^{\tau_\star} e_{n,i} e_{n,j}(\tau) d\tau)/(\sigma^2 \sigma_\varpi^2)$, $1 \leq i, j \leq n$, where σ_ϖ is the variance of the error on the studied parameter ϖ; the family of functions $(e_{n,i})_{i=1}^n$ is defined by (2.22)-(2.23)-(2.24); $\sigma = \max_{1 \leq i \leq n} \sigma_i^2$ where σ_i represents the *sensibility* of the response operator $\mathcal{R}$ with respect to a local perturbation $\Delta_{\bar{\mathsf{w}}}$ of the guess $\bar{\mathsf{w}}$ (see Fig. 9a):

$$\sigma_i^2 = \frac{1}{\mathsf{M}_{ii}^2 \Delta_{\bar{\mathsf{w}}}^2} \int_0^1 |\mathcal{R}(\bar{\mathsf{w}} + \Delta_{\bar{\mathsf{w}}} \mathsf{d}_i) - \mathcal{R}(\bar{\mathsf{w}})|^2(\mu) \, d\mu, \tag{6.5}$$

where d_i is the ith element of the canonical basis of $\mathbb{R}^n$ and $\mathsf{M}_{ii} = \int_0^{\tau_\star} e_{n,i}(\tau)^2 d\tau$. This work is more realistic than the one presented in the GRETA (because we consider a finite number p of observations) but it is still in development. Fig. 9b. shows the 100th iteration of a Kalman Filter type algorithm (Balakrishnan 1984) used to minimize Q effectively (in GRETA, we used also other algorithm). Each

iteration contains a Best Linear Unbiased Estimator step (BLUE step) where intervenes the linearized radiative transfer model (Tarantola 1987). For the model, we used the same data than in the numerical experiment section concerning the direct problem. We used $p = 300$ observations and we initialized the algorithm with a *constant guess*: $\bar{\mathsf{w}}_i = 0.5$, $1 \leq i \leq n = 29$. Moreover we set $\widetilde{\sigma} = 5 \times 10^{-4}$, $\sigma_{\varpi} = 0.1$, and $\Delta_{\bar{\mathsf{w}}} = 0.01$.

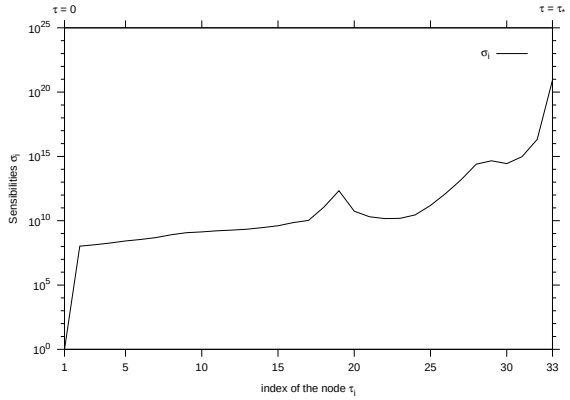

Fig. 9a. Local sensibilities (6.5) of the outgoing radiation specific intensity $\mathcal{R}(\bar{\mathsf{w}})$ with respect to local perturbations $\Delta_{\bar{\mathsf{w}}}$ on the guess $\bar{\mathsf{w}}$: $i \mapsto \sigma_i^2$.

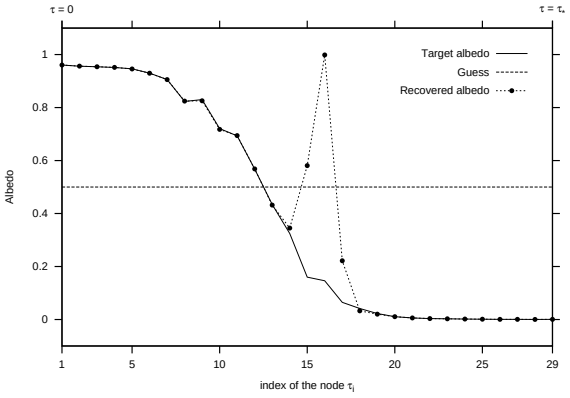

Fig. 9.b Recovering of the albedo by a numerical minimization of the quadratic error Q (6.4) — the measurement $\widetilde{I}_0^+$ of the outgoing radiation at the surface $\tau = 0$ is given by the Vernazza *et al.* (1981) NTLE model of the Sun atmosphere, $\lambda = 500$nm.

References

Ahues M., Largillier A. & Limaye B.V., *Spectral Computations for Bounded Operators*, Chapman and Hall/CRC, 2001.

Ahues M., D'Almeida F., Largillier A., Titaud O. & Vasconcelos P., An L^1 Refined Projection Approximate Solution of the Radiation Transfer Equation in Stellar Atmospheres, *J. Comput. Appl. Math.*, **140**(1&2): pp. 13–26, 2002, Elsevier Science.

Ahues M., D'Almeida F., Largillier A., Titaud O. & Vasconcelos P., Iterative reffinement schemes for an ill-conditioned transfer equation in Astrophysics, in: J. Levesley *et al.* (Eds.), Proceedings of Algorithms For Approximation IV, Univ. of Huddersfield, pp. 70–77, 2002.

Ahues M., Largillier A. & Titaud O., The roles of weak singularity and the grid uniformity in the relative error bounds, *Numer. Funct. Anal. Optim.*, **22**(7&8): pp. 789-814, 2002.

Atkinson K.E., A Survey of Numerical Methods for the Solution of Fredholm Integral Equations of the Second Kind, SIAM Publications, 1976.

Bal G., Inverse problems for homogeneous transport equations. I. The one-dimensional case. *Inverse Problems*, **16**(4): pp. 997–1011, 2000.

Balakrishnan A.V., *Kalman Filter Theory*, University series in modern engineering, Springer-Verlag, New York, 1984.

Briggs W.L., Henson V.E. & McCormick S.F., *A multigrid tutorial*, SIAM, Philadelphia, PA, 2000. Second edition.

D'Almeida F., Titaud O. & Vasconcelos P., A numerical study of iterative refinement schemes for weakly singular integral equations, *Appl. Math. Lett.*, **18**(5): pp. 571–576, 2005.

Golub G.H. & Van Loan C.F., *Matrix Computation*, The John Hopkins University Press, 1996. Third edition.

Gradshteyn I.S. & Ryzhik I.M., *Table of integrals, series, & products*, Translated from the Russian. Academic Press, Inc., San Diego, CA, 2000. Sixth edition.

Higham N.J., *Accuracy and stability of Numerical Algorithms*, SIAM Publications, Philadelphia, P.A., 1996. Second edition.

Largillier A. & Titaud O., Product integration quadratures for the radiative transfer problem with Hopf's kernel, *Integral Methods in Science and Engineering (Banff, AB, 2000)*, pp. 143–148, Birkhäuser Boston, MA, 2002.

McCormick N.J., Inverse radiative transfer problem: A review, *Nuclear Science and Engineering*, **112**: pp. 185-198, 1992.

Mihalas D., *Stellar atmospheres*, Freeman and co, San Francisco, 1970, 1978.

Rutily B. & Bergeat J., The solution of the Schwarzschild-Milne integral equation in an homogeneous isotropically scattering plane-parallel medium, *Journal of Quantitative Spectroscopy & Radiative Transfer*, 51(**6**): pp. 823–841, 1994.

Rutily B. & Chevallier L., Why is it so difficult to solve the radiative transfer equation ?, in this volume.

Saad Y., *Iterative methods for sparse linear systems*, SIAM Publications, Philadelphia, P.A., 2003. Second edition.

Tarantola A., *Inverse problem theory*, Methods for data fitting and model parameter estimation, Elsevier Science Publishers B.V., Amsterdam, 1987.

Titaud O., *Analyse et résolution numérique de l'équation de transfert. Application aux atmosphères stellaires*, Thèse de doctorat, Université de Saint Étienne, France, 2001. Available at `http://tel.ccsd.cnrs.fr/documents/archives0/00/00/13/33/`.

Titaud O., Reduction of computation in the numerical resolution of a second kind weakly singular Fredholm equation, *Integral Methods in Science and Engineering (Saint Étienne 2002)*, pp. 255–260, Birkhäuser Boston, 2004.

Vernazza J.E., Avrett E.H. & Loeser R., Structure of the solar chromosphere. III. Models of the EUV brightness components of the quiet Sun, *The Astrophysical Journal. Supplement Series*, **45**: pp. 635-725, 1981.